

1 **Effect of mid-term drought on *Quercus pubescens* BVOCs** 2 **emissions seasonality and their dependence to light and/or** 3 **temperature**

4 Amélie Saunier¹, Elena Ormeño¹, Christophe Boissard², Henri Wortham³, Brice Temime-
5 Roussel³, Caroline Lecareux¹, Alexandre Armengaud⁴, Catherine Fernandez¹.

6 ¹Aix Marseille Univ, Univ Avignon, CNRS, IRD, IMBE, Marseille, France.

7 ²Laboratoire des Sciences du Climat et de l'Environnement, LSCE/IPSL, CEA-CNRS-UVSQ, Université Paris-
8 Saclay, F-91191 Gif-sur-Yvette, France.

9 ³Aix Marseille Univ, CNRS, LCE, Laboratoire de Chimie de l'Environnement, Marseille, France

10 ⁴ Air PACA, 146 rue Paradis, Bâtiment Le Noilly Paradis, 13294 Marseille, Cedex 06.

11 *Correspondence to:* Amélie Saunier (amelie.saunier@imbe.fr)

12 **Key words:** BVOCs, natural and amplified drought, season, light and temperature

13 **Abstract.** Biogenic volatile organic compounds (BVOCs) emitted by plants represent a large source of carbon
14 compounds released into the atmosphere where they account for precursors of tropospheric ozone and secondary
15 organic aerosols. Being directly involved in air pollution and indirectly in climate change, understanding what
16 factors drive BVOC emissions is a prerequisite for modelling their emissions and predict air pollution. The main
17 algorithms currently used to model BVOCs emissions are mainly light and/or temperature dependent. Additional
18 factors such as seasonality and drought also influence isoprene emissions, especially in the Mediterranean region
19 which is characterized by a rather long drought period in summer. These factors are increasingly included in
20 models but only for the principal studied BVOC, namely isoprene but there are still some discrepancies in
21 estimations of emissions. In this study, the main BVOCs emitted by *Quercus pubescens*: isoprene, methanol,
22 acetone, acetaldehyde, formaldehyde, MACR, MVK and ISOPOOH (these 3 last compounds detected under the
23 same ion), were monitored with a PTR-ToF-MS over an entire seasonal cycle, under both *in situ* natural and
24 amplified drought which is expected with climate change. Amplified drought impacted all studied BVOCs by
25 reducing emissions in spring and summer while increasing emissions in autumn. All six BVOCs monitored showed
26 daytime light and temperature dependencies while three BVOCs (methanol, acetone and formaldehyde) also
27 showed emissions during the night despite the absence of light under constant temperature. Moreover, methanol
28 and acetaldehyde burst in the early morning and formaldehyde deposition/uptake were also punctually observed
29 which were not assessed by the classical temperature and light models.

30 **1 Introduction**

31 Plants contribute to global emissions of volatile organic compounds (VOCs) with an estimated emission rate of
32 10^{15} gC yr⁻¹ (Guenther *et al.* 1995; Harrison *et al.* 2013). The large variety of compounds released by plants
33 represents, at the global scale, 2-3% of the total carbon released in the atmosphere (Kesselmeier & Staudt 1999).
34 Under strong photochemical conditions, BVOCs, together with NO_x, can significantly contribute to tropospheric
35 ozone concentration (Xie *et al.* 2008; Papiez *et al.* 2009). In addition to its greenhouse effect, O₃ has strong effects
36 on plant metabolism (Reig-Armiñana *et al.* 2004; Beauchamp *et al.* 2005) as well as on human health (Lippmann
37 1989). BVOCs are also rapidly oxidized by OH radical and NO₃ (Hallquist *et al.* 2009; Liu *et al.* 2012), which
38 account for an important fraction of the total mass of secondary organic aerosols (SOA, Jimenez *et al.* 2009).
39 Methanol and acetone are, after isoprene, the principal BVOC released to the atmosphere. Isoprene emissions
40 represent between 400-600 TgC yr⁻¹ at the global scale (Arneeth *et al.* 2008) whereas methanol emissions vary
41 between 75 and 280 TgC yr⁻¹ (Singh *et al.* 2000; Heikes *et al.* 2002, respectively) and acetone emissions represent
42 only 33 TgC yr⁻¹ (Jacob *et al.* 2002). Other compounds such as acetaldehyde, methacrolein (MACR), methyl vinyl
43 ketone (MVK), isoprene hydroxy hydroperoxides (ISOPOOH) and formaldehyde, whose biogenic origin has been
44 poorly investigated, are better known to be anthropogenic and/or secondary VOCs issued from atmospheric
45 oxidations (Hallquist *et al.* 2009). However, acetaldehyde is also a by-product of plant metabolism and its
46 emissions represent 23 Tg yr⁻¹ at the global scale (Millet *et al.* 2010). Formaldehyde, MACR, MVK and ISOPOOH
47 are released by plants through oxidations of methanol and isoprene, respectively, within leaves but they can have
48 other leaf precursors (Oikawa & Lerdau 2013). Thus, it is thereby important to model all this panel of BVOCs
49 emissions with the aim of predicting their effect on secondary atmospheric chemistry.

50 Current models allow to predict BVOCs emissions according to the type of vegetation, biomass density, leaf age,
51 specific emission factor for many vegetal species, as well as the impact of some environmental factors. Models,
52 such as the MEGAN (Guenther *et al.* 2006; Guenther *et al.* 2012) or CHIMERE (Menuet *et al.* 2014) model, include
53 at least two main algorithms that allow to model light and temperature emissions dependence (called *L+T*
54 algorithm afterwards) and a temperature dependent algorithm (called *T* algorithm afterwards), both described in
55 Guenther *et al.* (1995). The *L+T* algorithm is typically used for BVOCs emissions whose synthesis rapidly relies
56 on photosynthesis, and hence include *de novo* emissions. The *T* algorithm is used for BVOCs emissions that do
57 not directly rely on BVOCs synthesis when, for example, they originate from permanent large storage pools
58 (Ormeno *et al.* 2011). The dependence to light and/or temperature is well documented for isoprenoids (Owen *et al.*
59 2002; Rinne *et al.* 2002; Dindorf *et al.* 2006) but there is still a lack of knowledge about highly volatile BVOCs
60 (e.g. methanol, acetone, acetaldehyde). However, many of these compounds are very reactive in the atmosphere
61 (Hallquist *et al.* 2009) and, could be emitted in large quantities to the atmosphere at global scale. The
62 characterization of their emissions and sensitivity to light and/or temperature is, thus, necessary in order to obtain
63 reliable predictions of atmospheric processes in order not to miss this important part of the atmospheric reactivity.

64 Other factors than light and temperature can drive BVOCs emissions such as water stress. Most studies dealing
65 with BVOCs response to water stress have, however, focused on terpene-like compounds and have been carried
66 out after weeks of watering restriction or removal under controlled conditions (for a review, see studies cited in
67 Peñuelas and Staudt 2010). Considerable uncertainty remains in our understanding of emission mechanisms since
68 some works showed increases (Funk *et al.* 2004; Monson *et al.* 2007) or decreases of isoprene emissions
69 (Brüggemann & Schnitzler 2002; Fortunati *et al.* 2008) and there is a lack of knowledge on the impact of water
70 stress on highly BVOCs emissions. Moreover, the understanding of isoprene sensitivity and highly volatile BVOCs

71 to recurrent water stress (few years) under *in situ* conditions is clearly missing. Likewise, the capacity of current
72 L+T and T algorithms to predict emission shifts under different drought scenarios in the context of climate change
73 needs to be addressed for isoprene and highly volatile compounds. This is of especial interest for the Mediterranean
74 area where the most severe climatic scenario of the IPCC predicts an intensification of summer drought consisting
75 on a rain reduction that can locally reach 30%, an extension of the drought period as well as a temperature rise of
76 3.4°C, (Giorgi & Lionello 2008; IPCC 2013; Polade *et al.* 2014) for 2100.

77 In the present investigation, we aimed (i) to study the emission factors of each studied BVOC released by *Q.*
78 *pubescens*, including isoprene and highly volatile compounds that originate from plant metabolism under water
79 stress (ii) to test the performance of the L+T and T algorithms to predict isoprene and highly volatile BVOC
80 emissions over the seasonal cycle and under two recurrent water stress treatments. *Q. pubescens* was chosen as
81 vegetal model because this species is highly resistant to drought and well widespread in the Northern
82 Mediterranean area occupying 2 million ha (Quézel & Médail 2003). It also represents the major source of isoprene
83 emissions in the Mediterranean area and the second one at the European scale (Keenan *et al.* 2009).

84 2 Material and methods

85 2.1 Experimental site

86 Our study was performed at the O₃HP site (Oak Observatory at OHP, Observatoire de Haute Provence), located
87 60 km North of Marseille, France (5°42'44" E, 43°55'54" N), at an elevation of 650m above the sea level. The
88 O₃HP (955m²), free from direct human disturbance for 70 years, is a homogeneous forest mainly composed of *Q.*
89 *pubescens* (≈ 90 % of the biomass and ≈ 75 % of the trees) with a mean diameter of 1.3 m. The remaining 10 %
90 of the biomass is mostly represented by *Acer monspessulanum* trees, a very low isoprene-emitter species (Genard-
91 Zielinski *et al.* 2015). The O₃HP site was created in 2009 in order to study the impact of climate change on a *Q.*
92 *pubescens* forest. Using a rainfall exclusion device (an automated monitored roof deployed during chosen rain
93 events) set up over part of the O₃HP canopy, it was possible to reduce natural rain by 30% and to extend the
94 drought period in an attempt to mimic the current climatic model projections for 2100 (Giorgi & Lionello 2008;
95 IPCC 2013; Polade *et al.* 2014). Two plots were considered in the site; a plot receiving natural precipitation where
96 trees grew under natural drought (300m² surface, used as control plot) and a second plot submitted to amplified
97 drought (232m² surface). Rain exclusion on this latter plot started on May 2012 and was continuously applied
98 every year, principally, during the growth period. Ombrothermic diagrams indicate that the drought period was
99 extended for 2 months in 2012, 4 months in 2013 and 3 months in 2014 for amplified drought relative to natural
100 drought (Fig 1). Data on cumulative precipitation show that 35% of rain was excluded in 2012 (from 29 April from
101 to 27 October), 33.5% in 2013 (from 7 July from to 29 December), 35.5% in 2014 (from 8 April to 8 December).
102 This experimental set up involved a recurrent drought in the amplified drought plot. Sampling was performed at
103 the branch-scale at the top of the canopy during three campaigns from October 2013 to July 2014, covering an
104 entire seasonal cycle: in autumn (14 to 28 October 2013, 2nd year of amplified drought), in spring (12 to 19 May
105 2014, 3rd year of amplified drought) and in summer (13 to 25 July 2014, 3rd year of amplified drought). Spring,
106 summer and autumn campaigns corresponded to the end of leaf growth, leaf maturation and the beginning of the
107 leaf senescence, respectively. The same five trees per plot were selected and investigated throughout the study.

108 2.2 Branch scale-sampling methods

109 Two identical dynamic branch enclosures were used for sampling gas exchange (in terms of CO₂, H₂O and
110 BVOCs) as fully described in Genard-Zielinski *et al.* (2015) with some modifications. Branches were enclosed in
111 a ≈ 30L PTFE (polytetrafluoroethylene) frame closed by a 50μm thick PTFE film. One tree from natural and one
112 tree from amplified drought plot were analysed concomitantly during 1 or 2 days. Inlet air was introduced at
113 9L.min⁻¹, controlled by mass flow controllers (MFC, Bronkhorst), using a pump, inside, by PTFE (KNF
114 N840.1.2FT.18®, Germany) allowing for air renewal inside the chamber every ~ 3min. Ozone was removed from
115 inlet air by placing PTFE filters impregnated with sodium thiosulfate (Na₂S₂O₃) as described by Pollmann *et al.*
116 (2005), so that oxidation of BVOCs due to ozone within the enclosed atmosphere is negligible. The excess of air
117 humidity was removed using drierite. A PTFE fan ensured a rapid mixing of the chamber air and a slight positive
118 pressure within the enclosure enabled the PTFE film to be held away from leaves to minimise biomass damage.
119 Microclimate (temperature, relative humidity and photosynthetically active radiation or PAR) was continuously
120 (every minute) monitored by a data logger (LI-COR 1400®; Lincoln, NE, USA) with a relative humidity and
121 temperature probe placed inside the chamber (RHT probe, HMP60, Vaisala, Finland) and a quantum sensor (PAR,
122 LI-COR, PAR-SA 190®, Lincoln, NE, USA) placed outside the chamber. The climatic conditions in terms of PAR
123 and temperatures are summarized in Fig. S1 (in supplementary files) for each field campaigns. All air flow rates
124 were controlled by mass flow controllers (MFC, Bronkhorst) and all tubing lines were made of PTFE. Chambers
125 were installed the day before measurements and flushed overnight. Enclosed branches contained 8 to 12 leaves
126 corresponding to a range of 1.4 to 3.6 g of dry matter and 110 to 320 cm² of leaf surface, respectively.

127 2.3 Ecophysiological parameters

128 Exchange of CO₂ and H₂O from the enclosed branches was continuously (every min) measured using infrared gas
129 analysers (IRGA 840A®, LI-COR) concomitantly with BVOCs emission measurements (cf. 2.4). Gas exchange
130 values were averaged by taking into account all the data measured between 12h and 15h (local time). Net
131 photosynthesis (P_n , μmolCO₂ m⁻² s⁻¹) and stomatal conductance to water (G_w , mmolH₂O m⁻² s⁻¹) were calculated
132 using equations described by Von Caemmerer and Farquhar (1981) as used in Genard-Zielinski *et al.* (2015) (for
133 more details, see Appendix A, equations A1 to A4). Leaves from enclosed branches were directly collected after
134 gas exchange sampling to accurately measure leaf surface with a leaf area meter. P_n and G_w were hence expressed
135 in a leaf surface basis. After that, leaves were freeze-dried to assess their dry mass.

136 2.4 BVOCs analysis

137 A PTR-ToF-MS 8000 instrument (Ionicon Analytik GmbH, Innsbruck, Austria) was used for online measurements
138 of BVOCs emitted by the enclosed branches. A multi-position common outlet flow path selector valve system
139 (Vici) and a vacuum pump were used to sequentially select air samples from: amplified drought, inlet air, natural
140 drought, ambient air and catalyst. The catalyst consists in a 25 cm long stainless steel tubing, filled with platinum
141 wool and heated at 350°C to efficiently remove VOCs from sample and measure potential instrumental background
142 levels. Each sample was analysed every hour, with 15min of analysis. Mass spectra in the range 0-500amu were
143 recorded at 1min integration time. The reaction chamber pressure was fixed at 2.1mbar, the drift tube voltage at
144 550V and the drift tube temperature at 313 K corresponding to an electric field strength applied to the drift tube

145 (E) to a buffer gas density (N) ratio of 125Td (1Td = 10^{-17} V cm²). A calibration gas standard, consisting of a
146 mixture of 14 aromatic organic compounds (TO-14A Aromatic Mix, Restek Corporation, Bellefonte, USA, 100 ±
147 10ppb in Nitrogen), was used to experimentally determine the ion relative transmission efficiency. BVOCs
148 targeted in this study and their corresponding ions include formaldehyde (m/z 31.018), methanol (m/z 33.033),
149 acetaldehyde (m/z 45.03), acetone (m/z 59.05), isoprene (m/z 41.038, 69.069) and MACR+MVK+ISOPOOH (m/z
150 71.049, these three compounds were detected with the same ion with PTR-MS). The signal corresponding to
151 protonated VOCs was converted into mixing ratios by using the proton transfer rate constants *k* given by Cappellin
152 *et al.* (2012). Formaldehyde concentrations were calculated according to the method described by Vlasenko *et al.*
153 (2010) to account for its humidity dependent sensitivity.

154 BVOCs emissions rates (ER) were calculated by considering the BVOCs concentrations in the inlet and outlet air
155 as follows (equation 1):

$$156 \quad ER = \frac{Q_0 * (C_{out} - C_{in})}{B} \quad (1)$$

157 where *ER* was expressed in $\mu\text{gC g}_{\text{DM}}^{-1} \text{h}^{-1}$, Q_0 was the flow rate of the air introduced into the chamber (L h^{-1}), C_{out}
158 and C_{in} were the concentrations in the inflowing and outflowing air ($\mu\text{gC L}^{-1}$), respectively, and *B* was the total
159 dry biomass matter (g_{DM}). Daily cycles were made by averaging measured emissions of all trees every hour.

160 2.5 Emission algorithms

161 The light and/or temperature dependence of *Q. pubescens* BVOCs (isoprene and highly volatile compounds) under
162 natural and amplified drought was tested using both the *L+T* and *T* algorithms. Emission rates calculated according
163 to these algorithms (afterwards, called ER_{L+T} and ER_T , respectively) were calculated using the equations described
164 in Guenther *et al.* (1995) (for more details, see Appendix B, equations B1 to B5). The empirical coefficient β (used
165 in the *T* algorithm) was determined for each compound according to the season and the treatment through the slope
166 of correlation between the natural logarithm of emissions rates (measured emissions, $\mu\text{gC g}_{\text{DM}}^{-1} \text{h}^{-1}$) and
167 experimental temperature (K). Emissions factors (*EF*), that are emissions rates at standard conditions of light and
168 temperature, $1000\mu\text{mol m}^{-2} \text{s}^{-1}$ and 30°C), were used to calculate modelled emissions and were determined for each
169 compound under each season and treatment tree by tree. *EF* values correspond to the slope of the correlation
170 between experimental emission rates and $C_l * C_t$ when using the *L+T* algorithm or C_T when using the *T* algorithm
171 (without forcing data to pass through the origin, see Appendix B for a full description of $C_l * C_t$ and C_T). R^2 and *p*-
172 value of these correlations tree by tree are presented in tables S1 – S6 (supplementary files) and all parameters
173 used for the calculation of modelled emissions are presented in tables S7 and S8 (for $C_l * C_t$ and C_T , respectively,
174 in supplementary files).

175 2.6 Data treatment

176 Data treatment was performed with the software STATGRAPHICS® centurion XV (Statpoint, Inc). After having
177 checked the normality of the data set, two-way repeated measures ANOVA were carried out to evaluate the
178 variability of *Pn*, *Gw* and BVOC emission rates according to the drought treatment and season. Correlation
179 coefficient (R^2) and slope (called “*sl*” afterwards) from Pearson's correlations between measured and modelled
180 emissions were used to evaluate the algorithm (*L+T* or *T*) that better predicted *Q. pubescens* emissions under the
181 different drought conditions and seasonal cycle. The slope of those correlations indicate if there was an under- or

182 over- estimation of modelled emissions when $sl < 1$ and $sl > 1$, respectively. For that, slope comparison tests were
183 performed to check for slope significant differences from 1. These correlations were obtained without forcing data
184 to pass through the origin and with this relation: modelled emissions = $a \cdot \text{measured emission} + b$.

185 **3. Results and discussion**

186 **3.1 Ecophysiological parameters**

187 The physiology of *Q. pubescens* was slightly impacted by amplified drought over the whole study (Fig. 2), with a
188 decrease of G_w under amplified drought compared to natural drought – ranging from 44 % in spring ($P < 0.1$) to
189 55 % in summer ($P < 0.01$, Table 1). In autumn, there was no significant difference between both treatments. P_n
190 was only slightly reduced in summer by 36 % ($P < 0.1$) with no difference for the others season. Thus, the stomatal
191 closure observed had a slight impact on carbon assimilation. Indeed, *Q. pubescens* has a high stem hydraulic
192 efficiency (Nardini & Pitt 1999) which compensates stomatal closure since it allows to use water more efficiently,
193 thus, maintaining P_n . Moreover, it must be noted that an increase of P_n was observed in autumn and could likely
194 be attributed to autumnal rains. These results showed that the amplified drought artificially applied to *Q. pubescens*
195 at O₃HP led to a moderate drought for this species, based on a moderate reduction of the physiological
196 performances (Niinemets 2010).

197 **3.2 Effect of drought on BVOCs emissions**

198 Emissions of all BVOCs followed during this experimentation were reduced under amplified drought compared
199 to natural drought, especially in spring and summer (Table 1) except for acetaldehyde emissions. Indeed,
200 acetaldehyde was not significantly different between both treatments probably due to a large variability of the data
201 set. In autumn, for all BVOCs, there was no difference between both plots. The decrease of oxygenated BVOCs
202 in spring and summer under amplified drought (e.g. methanol, MACR+MVK+ISOPOOH, formaldehyde, acetone)
203 could be explained by stomatal closure in spring and summer under amplified drought since emissions of these
204 compounds are strongly bound to G_w (Niinemets *et al.* 2004). Isoprene emissions were also reduced in spring and
205 summer during the 3rd year of this experiment whereas an increase had been observed in the first year (Génard-
206 Zielinski *et al.* in prep) as well as what had been shown by Brüggemann and Schnitzler (2002) but this work was
207 conducted with potted plants. The isoprene decrease observed in our experiment cannot be explained by the
208 stomatal closure because this compound could also be emitted through the cuticle (Sharkey & Yeh 2001). It could
209 rather be due to the decrease of P_n which reduced the carbon availability to produce isoprene. Moreover, carbon
210 assimilated through P_n can be also invested into the synthesis of other defense compounds leading to a decrease
211 of isoprene production and emission.

212 **3.3 Effect of drought on light and/or temperature dependence through a seasonal cycle**

213 All six BVOCs monitored showed daytime light and temperature dependencies (isoprene, degradation products of
214 isoprene and acetaldehyde), while three BVOCs (methanol, acetone and formaldehyde) also showed emissions
215 during the night despite the absence of light under constant temperature.

216

217 Regarding the light and temperature dependencies, the daily cycle of isoprene emissions (Fig. 3) showed that this
218 compound clearly responds to light and temperature as already known (Guenther *et al.* 1993) and that this response
219 is not impacted by amplified drought. Isoprene can protect thylakoids from oxidative damage (Velikova *et al.*
220 2011) occurring mainly during the day which can explain this kind of dependence. Yet, our results show the
221 intensity of isoprene emission factor under natural and amplified drought is very different independently of the
222 season. The modelled emissions were roughly very representative of measured emissions. We note, however, that
223 in spring, under natural drought, emissions were slightly underestimated ($sl = 0.84$, $P < 0.05$, $R^2 = 0.90$). It suggests
224 that although light and temperature remain the main factors driving isoprene emissions in spring but other
225 parameters explain 10% of these emissions. At this season, plants likely needed to produce more isoprene to protect
226 the establishment of photosynthetic machinery in the new leaves which could slightly modify the effects of light
227 and temperature on isoprene emissions.

228 MACR+MVK+ISOPOOH emissions, as isoprene, seemed to respond better to light and temperature than to only
229 temperature (Fig. S2 in supplementary files) since correlations between measured emissions and ER_{L+T} were
230 always better than correlations with ER_T . Since MACR+MVK+ISOPOOH are oxidation products of isoprene
231 (Oikawa & Lerdau 2013), it is not surprising that these compounds followed the same pattern than isoprene in
232 terms of dependence to light and temperature. The estimations of ER_{L+T} were quite good except in spring under
233 natural drought where a slight underestimation was observed ($sl = 0.87$, $P < 0.05$). This underestimation can be
234 explain by the underestimation of isoprene emissions observed at the same time since MACR+MVK+ISOPOOH
235 comes from isoprene oxidation.

236 The dependence of acetaldehyde emissions to light and/or temperature is very contrasted; studies have shown that
237 they are bound to both light and temperature (Jardine 2008; Fares *et al.* 2011) or to temperature only (Hayward *et*
238 *al.* 2004). Our results suggested that acetaldehyde emissions were mainly bound to light and temperature (Fig. 4).
239 Indeed, correlations between measured and ER_{L+T} were always better than with ER_T . However, some discrepancies
240 were observed. Under natural drought, underestimations were observed in spring and summer ($sl = 0.72$, and $sl =$
241 0.57 , $P < 0.05$, respectively) whereas in autumn, there was a good estimation ($sl = 0.86$, $P > 0.05$). Under amplified
242 drought, underestimation was only observed in summer ($sl = 0.80$, $P < 0.05$). Trees studied in this experiment did
243 not show the same dependence to light and temperature for acetaldehyde emissions. R^2 of the correlation
244 determining EF (performed tree by tree), varies from 0.34 to 0.90 in summer, from 0.67 to 0.92 in spring, under
245 natural drought. Under amplified drought, R^2 varies from 0.22 to 0.83 in summer (Tables S6 in supplementary
246 files). These results suggest that the effect of light and temperature on acetaldehyde emissions strongly depend on
247 tree considered and could explain the underestimations observed in our experiment. Moreover, daily cycles of
248 acetaldehyde emissions presented also an emissions burst in the morning (at 7h, local time) in spring (under both
249 treatments) and in summer (only under natural drought). Acetaldehyde can be produced due to an overflow of
250 pyruvic acid during light-dark transitions. Cytosolic pyruvic acid levels rise rapidly and it can be converted into
251 acetaldehyde by pyruvate decarboxylase (Fall 2003). This mechanism could explain the morning burst for this
252 compound and the fact that no emissions during the night was observed.

253
254 We observed emissions of methanol, acetone and formaldehyde during the night under no light and constant
255 temperature (around 20°C, see supplementary files S1). Correlations between ER_{L+T} or ER_T and measured
256 methanol emissions were very similar especially in spring and summer (Fig. 5). However, some observed

257 phenomena suggested that methanol emission was sustained by temperature in the absence of light. Indeed, the
258 burst in the early morning (at 7h, local time), similar to acetaldehyde, was observed when stomata opened in spring
259 and summer, independently of the drought treatment although it was clearer under natural than amplified drought.
260 This burst can be explained by a strong release of this compound that has been accumulated in the intercellular air
261 space and leaf liquid pools (due to the relative high polarity of methanol) at night when stomata are closed (Hüve
262 *et al.* 2007). Moreover, for both drought treatments, methanol emissions during the night were observed at any
263 seasons (especially autumn) which could be explained by nocturnal temperatures (roughly constant) that sufficed
264 to maintain the biochemical processes involved in methanol formation. Methanol emissions, which result from the
265 demethylation of pectin during the leaf elongation, has already been described to be temperature dependent alone
266 (Hayward *et al.* 2004; Folkers *et al.* 2008). However, our results suggest that methanol emissions respond strongly
267 to light and temperature during the day. This kind of diurnal emissions cycle has already been described by Smiatek
268 and Steinbrecher (2006). Our results about daily cycles of acetone emissions (Fig. S3 in supplementary files)
269 showed that this compound responded better to light and temperature than only temperature since correlations
270 were better with ER_{L+T} . Under natural drought, the modelled emissions were well representative of measured
271 emissions in summer. By contrast, in spring and in autumn, slight underestimations were observed ($sl = 0.88$, $P <$
272 0.05 and $sl = 0.69$, $P < 0.05$, respectively). Under amplified drought, good estimations were observed in summer
273 and autumn but in spring, there was an overestimation of modelled emissions ($sl = 1.27$, $P < 0.05$). Previous studies
274 have shown that acetone rather depends on temperature alone (Fares *et al.* 2011) or to light and temperature (Jacob
275 *et al.* 2002), indicating that its dependence on light and/or temperature remains unclear. During the day, acetone
276 emissions were dependent on light and temperature and emissions still occurred during the night, especially in
277 autumn. Alike methanol, nocturnal temperatures could allow to maintain acetone formation (Smiatek &
278 Steinbrecher 2006). Acetone is a by-product of plant metabolism (Jacob *et al.* 2002) and its production can be
279 enzymatic and non-enzymatic (Fall 2003) which can explain these observed differences through the day. We can
280 suppose that acetone emissions observed during the day could come from the enzymatic activity and, on the
281 contrary, during the night, they could come from the non-enzymatic production.

282 Formaldehyde emissions followed the same pattern than methanol and acetone emissions (Fig. S4 in
283 supplementary files), especially in autumn. By considering only the daytime (correlation with $L+T$ modelled
284 emissions), there were good estimations in summer and autumn and a slight underestimation was observed in
285 spring ($sl = 0.89$, $P < 0.05$) for natural drought. Under amplified drought, correlations indicated that $L+T$ modelled
286 emissions were well representative of measured emissions, but some negative emissions were observed in summer
287 which suggested a deposition or an uptake of this compound by leaves as already highlighted by Seco *et al.* (2008).
288 This phenomenon could have a role in stress tolerance, since formaldehyde can be catabolised (mainly through
289 oxidations) within leaves leading to CO_2 formation (Oikawa & Lerdau 2013). Emissions during the night suggest
290 that formaldehyde came from another source than oxidation within leaves since oxidations occur mainly during
291 the day due to an excess of light in chloroplasts, principal place of reactive oxygen species production (Asada
292 2006). Thus, formaldehyde emissions observed during the night could result from, for example, the glyoxylate
293 decarboxylation or the dissociation of 5,10-methylene-THF (Oikawa & Lerdau 2013).

294 Predicting emissions rates of these 3 compounds (methanol, acetone and formaldehyde), during the night, seem to
295 require other parameters such as a temperature threshold, below which methanol, acetone and formaldehyde
296 synthesis and so emissions do not occur.

297 4 Conclusion

298 After 3 years of amplified drought, all BVOC emissions were reduced in spring and summer compared to natural
299 drought whereas, in autumn, an increase was observed for some compounds. These results are in opposition with
300 the results obtained after only one year of amplified drought (2012), especially for isoprene, where an increase
301 was observed for this compound (Génard-Zielinski *et al.* in prep). Amplified drought did not seem to shift the
302 dependence to light and/or temperature which remained unchanged between treatments.
303 Moreover, two different dependence behaviours were found: (i) all six BVOCs monitored showed daytime light
304 and temperature dependencies while (ii) only three BVOCs (methanol, acetone and formaldehyde) also showed
305 that their emissions were maintained during the night with no light at rather constant nocturnal temperatures.
306 Moreover, some phenomena, such as methanol and acetaldehyde emissions bursts in early morning or the
307 formaldehyde deposition/uptake (formaldehyde), were not assessed by either $L+T$ or T algorithm.

308 Appendix A: calculation of ecophysiological parameters

309 Net photosynthesis (P_n , $\mu\text{molCO}_2 \text{ m}^{-2} \text{ s}^{-1}$) was calculated using equations described by Von Caemmerer and
310 Farquhar (1981) as follows:

$$311 \quad P_n = \frac{F*(Cr-C_s)}{S} - C_s * E \quad (\text{A1})$$

312 Where F is the inlet air flow (mol s^{-1}), C_s and C_r are the sample and reference CO_2 molar fraction respectively
313 (ppm), S is the leaf surface (m^2), $C_s * E$ is the fraction of CO_2 diluted in water evapotranspiration and E (molH_2O
314 $\text{m}^{-2} \text{ s}^{-1}$ then transformed in $\text{mmolH}_2\text{O m}^{-2} \text{ s}^{-1}$, afterward) is the transpiration rate calculated as follow:

$$315 \quad E = \frac{F*(W_s-W_r)}{S*(1-W_s)} \quad (\text{A2})$$

316 where W_s and W_r are the sample and the reference H_2O molar fraction respectively ($\text{molH}_2\text{O mol}^{-1}$).

317 Stomatal conductance to water (G_w , $\text{molH}_2\text{O m}^{-2} \text{ s}^{-1}$ then transformed in $\text{mmolH}_2\text{O m}^{-2} \text{ s}^{-1}$) was calculated using
318 the following equation:

$$319 \quad G_w = \frac{E*(1-\frac{W_l-W_s}{2})}{W_l-W_s} \quad (\text{A3})$$

320 where W_l is the molar concentration of water vapour within the leaf ($\text{molH}_2\text{O mol}^{-1}$) calculated as follows:

$$321 \quad W_l = \frac{V_{psat}}{P} \quad (\text{A4})$$

322 where V_{psat} is the saturated vapour pressure (kPa) and P was the atmospheric pressure (kPa).

323 Appendix B: Modelled emissions calculation

324 The modelled emissions rates according to light and temperature (ER_{L+T}) or the temperature algorithm (ER_T) were
325 calculated according to algorithms described in Guenther *et al.* (1995) as follows :

$$326 \quad ER_{L+T} = EF_{L+T} * C_l * C_t \quad (\text{B1})$$

327 where EF_{L+T} is the emission factor at $1000 \mu\text{mol m}^{-2} \text{s}^{-1}$ of photosynthetically active radiation (PAR) and 30°C of
328 temperature (obtained with the slope of the correlation between experimental emissions and $C_l * C_t$ without forcing
329 data to pass through the origin), C_l and C_t correspond to light and temperature dependence factors respectively and
330 were calculated with the following formulae:

$$331 \quad C_l = \frac{\alpha C_{L1} L}{\sqrt{1 + \alpha^2 L}} \quad (\text{B2})$$

$$332 \quad C_t = \frac{\exp\left(\frac{C_{T1}(T - T_S)}{RT_S T}\right)}{1 + \exp\left(\frac{C_{T2}(T - T_M)}{RT_S T}\right)} \quad (\text{B3})$$

333 where $\alpha = 0.0027$, $C_{L1} = 1.066$, $C_{T1} = 95000 \text{J mol}^{-1}$, $C_{T2} = 230000 \text{J mol}^{-1}$, $T_M = 314 \text{K}$ are empirically derived
334 constants, L is the photosynthetically active radiation (PAR) flux ($\mu\text{mol m}^{-2} \text{s}^{-1}$), T is the leaf experimental
335 temperature (K) and T_S is the leaf temperature at standard condition (303K).

336 Modelled emissions according to temperature alone that is ER_T , was calculated as follows:

$$337 \quad ER_T = EF_T * C_T \quad (\text{B4})$$

338 where EF_T is the emission factor at 30°C of temperature (obtained with the slope of the correlation between
339 experimental emissions and C_T without forcing data to pass through the origin) and C_T is a temperature dependence
340 factor calculated as follows:

$$341 \quad C_T = \exp[\beta(T - T_S)] \quad (\text{B5})$$

342 where β is an empirical coefficient (with a standard variation value of 0.09K^{-1} used in literature when not measured)
343 determined, in this study, for each compound according to the season and the treatment through the slope of the
344 correlation between the natural logarithm of measured emissions rates (ER , $\mu\text{gC g}_{\text{DM}}^{-1} \text{h}^{-1}$) and experimental
345 temperature (expressed in K), T is the leaf experimental temperature (K) and T_S is the standard temperature (303K).

346 **Author contribution**

347 AS, EO and CF designed the research and the experimental design. AS, BTR, EO and CF conducted the research.
348 AS, CB, BTR, and CL collected and analyzed the data. AS, EO, CB, HW, BTR, AA and CF wrote the manuscript

349 **Competing interests**

350 The authors declare that they have no conflict of interest.

351 **Acknowledgments**

352 This work was supported by the French National Agency for Research (ANR) through the SecPriMe² project
353 (ANR-12-BSV7-0016-01); Europe (FEDER) and ADEME/PACA for PhD funding. We are grateful to FR3098
354 ECCOREV for the O₃HP facilities (<https://o3hp.obs-hp.fr/index.php/fr/>). We are very grateful to J.-P. Orts, I.
355 Reiter. We also thank all members of the DFME team from IMBE and particularly: S. Greff, S. Dupouyet and A.
356 Bousquet-Melou for their help during measurements and analysis. We thank also, the Université Paris Diderot-
357 Paris7 for its support. The authors thank the MASSALYA instrumental platform (Aix Marseille Université,
358 lce.univ-amu.fr) for the analysis and measurements used in this publication.

- 360 Arneth A., Monson R., Schurgers G., Niinemets Ü. & Palmer P. (2008). Why are estimates of global terrestrial
361 isoprene emissions so similar (and why is this not so for monoterpenes)? *Atmospheric Chemistry and*
362 *Physics*, 8, 4605-4620.
- 363 Asada K. (2006). Production and scavenging of reactive oxygen species in chloroplasts and their functions. *Plant*
364 *physiology*, 141, 391-396.
- 365 Beauchamp J., Wisthaler A., Hansel A., Kleist E., Miebach M., NIINEMETS Ü., Schurr U. & WILDT J. (2005).
366 Ozone induced emissions of biogenic VOC from tobacco: relationships between ozone uptake and
367 emission of LOX products. *Plant, Cell & Environment*, 28, 1334-1343.
- 368 Brüggemann N. & Schnitzler J.P. (2002). Comparison of Isoprene Emission, Intercellular Isoprene
369 Concentration and Photosynthetic Performance in Water-Limited Oak (*Quercus pubescens* Willd. and
370 *Quercus robur* L.) Saplings. *Plant Biology*, 4, 456-463.
- 371 Cappellin L., Karl T., Probst M., Ismailova O., Winkler P.M., Soukoulis C., Aprea E., Märk T.D., Gasperi F. &
372 Biasioli F. (2012). On quantitative determination of volatile organic compound concentrations using
373 proton transfer reaction time-of-flight mass spectrometry. *Environmental science & technology*, 46,
374 2283-2290.
- 375 Dindorf T., Kuhn U., Ganzeveld L., Schebeske G., Ciccioli P., Holzke C., Köble R., Seufert G. & Kesselmeier J.
376 (2006). Significant light and temperature dependent monoterpene emissions from European beech
377 (*Fagus sylvatica* L.) and their potential impact on the European volatile organic compound budget.
378 *Journal of Geophysical Research: Atmospheres*, 111.
- 379 Fall R. (2003). Abundant oxygenates in the atmosphere: a biochemical perspective. *Chemical reviews*, 103,
380 4941-4952.
- 381 Fares S., Gentner D.R., Park J.-H., Ormeno E., Karlik J. & Goldstein A.H. (2011). Biogenic emissions from
382 Citrus species in California. *Atmospheric Environment*, 45, 4557-4568.
- 383 Folkers A., Hüve K., Ammann C., Dindorf T., Kesselmeier J., Kleist E., Kuhn U., Uerlings R. & Wildt J. (2008).
384 Methanol emissions from deciduous tree species: dependence on temperature and light intensity. *Plant*
385 *biology*, 10, 65-75.
- 386 Fortunati A., Barta C., Brilli F., Centritto M., Zimmer I., Schnitzler J.P. & Loreto F. (2008). Isoprene emission is
387 not temperature - dependent during and after severe drought - stress: a physiological and biochemical
388 analysis. *The Plant Journal*, 55, 687-697.
- 389 Funk J., Mak J. & Lerdau M. (2004). Stress - induced changes in carbon sources for isoprene production in
390 *Populus deltoides*. *Plant, Cell & Environment*, 27, 747-755.
- 391 Genard-Zielinski A.-C., Boissard C., Fernandez C., Kalogridis C., Lathièrre J., Gros V., Bonnaire N. & Ormeño
392 E. (2015). Variability of BVOC emissions from a Mediterranean mixed forest in southern France with a
393 focus on *Quercus pubescens*. *Atmospheric Chemistry and Physics Discussions*, 14, 17225-17261.
- 394 Giorgi F. & Lionello P. (2008). Climate change projections for the Mediterranean region. *Global and Planetary*
395 *Change*, 63, 90-104.
- 396 Guenther A., Hewitt C.N., Erickson D., Fall R., Geron C., Graedel T., Harley P., Klinger L., Lerdau M., McKay
397 W.A., Pierce T., Scholes B., Steinbrecher R., Tallamraju R., Taylor J. & Zimmerman P. (1995). A
398 global model of natural volatile organic compound emissions. *Journal of Geophysical Research:*
399 *Atmospheres*, 100, 8873-8892.
- 400 Guenther A., Jiang X., Heald C., Sakulyanontvittaya T., Duhl T., Emmons L. & Wang X. (2012). The Model of
401 Emissions of Gases and Aerosols from Nature version 2.1 (MEGAN2. 1): an extended and updated
402 framework for modeling biogenic emissions.
- 403 Guenther A., Karl T., Harley P., Wiedinmyer C., Palmer P. & Geron C. (2006). Estimates of global terrestrial
404 isoprene emissions using MEGAN (Model of Emissions of Gases and Aerosols from Nature).
405 *Atmospheric Chemistry and Physics*, 6, 3181-3210.
- 406 Guenther A.B., Zimmerman P.R., Harley P.C., Monson R.K. & Fall R. (1993). Isoprene and monoterpene
407 emission rate variability: model evaluations and sensitivity analyses. *Journal of Geophysical Research:*
408 *Atmospheres (1984–2012)*, 98, 12609-12617.
- 409 Hallquist M., Wenger J., Baltensperger U., Rudich Y., Simpson D., Claeys M., Dommen J., Donahue N., George
410 C. & Goldstein A. (2009). The formation, properties and impact of secondary organic aerosol: current
411 and emerging issues. *Atmospheric Chemistry and Physics*, 9, 5155-5236.
- 412 Harrison S.P., Morfopoulos C., Dani K., Prentice I.C., Arneth A., Atwell B.J., Barkley M.P., Leishman M.R.,
413 Loreto F. & Medlyn B.E. (2013). Volatile isoprenoid emissions from plastid to planet. *New Phytol.*,
414 197, 49-57.
- 415 Hayward S., Tani A., Owen S.M. & Hewitt C.N. (2004). Online analysis of volatile organic compound emissions
416 from Sitka spruce (*Picea sitchensis*). *Tree Physiology*, 24, 721-728.

417 Heikes B.G., Chang W., Pilson M.E., Swift E., Singh H.B., Guenther A., Jacob D.J., Field B.D., Fall R. &
418 Riemer D. (2002). Atmospheric methanol budget and ocean implication. *Global Biogeochemical*
419 *Cycles*, 16, 80-1-80-13.

420 Hüve K., Christ M., Kleist E., Uerlings R., Niinemets Ü., Walter A. & Wildt J. (2007). Simultaneous growth and
421 emission measurements demonstrate an interactive control of methanol release by leaf expansion and
422 stomata. *Journal of experimental botany*, 58, 1783-1793.

423 IPCC (2013). In: *Contribution of working group I to the fifth assessment report of the intergovernmental panel on*
424 *climate change*. Cambridge University Press Cambridge.

425 Jacob D.J., Field B.D., Jin E.M., Bey I., Li Q., Logan J.A., Yantosca R.M. & Singh H.B. (2002). Atmospheric
426 budget of acetone. *Journal of Geophysical Research: Atmospheres (1984–2012)*, 107, ACH 5-1-ACH
427 5-17.

428 Jardine J. (2008). Plant physiological and environmental controls over the exchange of acetaldehyde between
429 forest canopies and the atmosphere. *Biogeosciences*, 5.

430 Jimenez J., Canagaratna M., Donahue N., Prevot A., Zhang Q., Kroll J.H., DeCarlo P.F., Allan J.D., Coe H. &
431 Ng N. (2009). Evolution of organic aerosols in the atmosphere. *Science*, 326, 1525-1529.

432 Keenan T., Niinemets Ü., Sabate S., Gracia C. & Peñuelas J. (2009). Process based inventory of isoprenoid
433 emissions from European forests: model comparisons, current knowledge and uncertainties.
434 *Atmospheric Chemistry and Physics Discussions*, 9, 6147-6206.

435 Kesselmeier J. & Staudt M. (1999). Biogenic volatile organic compounds (VOC): an overview on emission,
436 physiology and ecology. *Journal of Atmospheric Chemistry*, 33, 23-88.

437 Lippmann M. (1989). Health effects of ozone a critical review. *Japca*, 39, 672-695.

438 Liu Y., Siekmann F., Renard P., El Zein A., Salque G., El Haddad I., Temime-Roussel B., Voisin D., Thissen R.
439 & Monod A. (2012). Oligomer and SOA formation through aqueous phase photooxidation of
440 methacrolein and methyl vinyl ketone. *Atmospheric Environment*, 49, 123-129.

441 Menut L., Bessagnet B., Khvorostyanov D., Beekmann M., Blond N., Colette A., Coll I., Curci G., Foret G. &
442 Hodzic A. (2014). CHIMERE 2013: a model for regional atmospheric composition modelling.
443 *Geoscientific Model Development*, 6, 981-1028.

444 Millet D.B., Guenther A., Siegel D.A., Nelson N.B., Singh H.B., de Gouw J.A., Warneke C., Williams J.,
445 Eerdekens G. & Sinha V. (2010). Global atmospheric budget of acetaldehyde: 3-D model analysis and
446 constraints from in-situ and satellite observations. *Atmospheric Chemistry and Physics*, 10, 3405-3425.

447 Monson R.K., Trahan N., Rosenstiel T.N., Veres P., Moore D., Wilkinson M., Norby R.J., Volder A., Tjoelker
448 M.G. & Briske D.D. (2007). Isoprene emission from terrestrial ecosystems in response to global
449 change: minding the gap between models and observations. *Philosophical Transactions of the Royal*
450 *Society of London A: Mathematical, Physical and Engineering Sciences*, 365, 1677-1695.

451 Nardini A. & Pitt F. (1999). Drought resistance of *Quercus pubescens* as a function of root hydraulic
452 conductance, xylem embolism and hydraulic architecture. *New Phytol.*, 143, 485-493.

453 Niinemets Ü. (2010). Mild versus severe stress and BVOCs: thresholds, priming and consequences. *Trends in*
454 *plant science*, 15, 145-153.

455 Niinemets Ü., Loreto F. & Reichstein M. (2004). Physiological and physicochemical controls on foliar volatile
456 organic compound emissions. *Trends in plant science*, 9, 180-186.

457 Oikawa P.Y. & Lerdau M.T. (2013). Catabolism of volatile organic compounds influences plant survival. *Trends*
458 *in plant science*, 18, 695-703.

459 Ormeno E., Goldstein A. & Niinemets Ü. (2011). Extracting and trapping biogenic volatile organic compounds
460 stored in plant species. *TrAC Trends in Analytical Chemistry*, 30, 978-989.

461 Owen S., Harley P., Guenther A. & Hewitt C. (2002). Light dependency of VOC emissions from selected
462 Mediterranean plant species. *Atmospheric environment*, 36, 3147-3159.

463 Papiez M.R., Potosnak M.J., Goliff W.S., Guenther A.B., Matsunaga S.N. & Stockwell W.R. (2009). The
464 impacts of reactive terpene emissions from plants on air quality in Las Vegas, Nevada. *Atmospheric*
465 *Environment*, 43, 4109-4123.

466 Polade S.D., Pierce D.W., Cayan D.R., Gershunov A. & Dettinger M.D. (2014). The key role of dry days in
467 changing regional climate and precipitation regimes. *Scientific reports*, 4.

468 Pollmann J., Ortega J. & Helmig D. (2005). Analysis of atmospheric sesquiterpenes: Sampling losses and
469 mitigation of ozone interferences. *Environmental science & technology*, 39, 9620-9629.

470 Quézel P. & Médail F. (2003). *Ecologie et biogéographie des forêts du bassin méditerranéen*. Elsevier Paris.

471 Reig-Armiñana J., Calatayud V., Cerveró J., García-Breijo F., Ibars A. & Sanz M. (2004). Effects of ozone on
472 the foliar histology of the mastic plant (*Pistacia lentiscus* L.). *Environmental Pollution*, 132, 321-331.

473 Rinne H., Guenther A., Greenberg J. & Harley P. (2002). Isoprene and monoterpene fluxes measured above
474 Amazonian rainforest and their dependence on light and temperature. *Atmospheric Environment*, 36,
475 2421-2426.

476 Seco R., Penuelas J. & Filella I. (2008). Formaldehyde emission and uptake by Mediterranean trees *Quercus ilex*
477 and *Pinus halepensis*. *Atmospheric Environment*, 42, 7907-7914.

478 Sharkey T.D. & Yeh S. (2001). Isoprene emission from plants. *Annual review of plant biology*, 52, 407-436.

479 Singh H., Chen Y., Tabazadeh A., Fukui Y., Bey I., Yantosca R., Jacob D., Arnold F., Wohlfrom K. & Atlas E.
480 (2000). Distribution and fate of selected oxygenated organic species in the troposphere and lower
481 stratosphere over the Atlantic. *Journal of Geophysical Research: Atmospheres (1984–2012)*, 105, 3795-
482 3805.

483 Smiatek G. & Steinbrecher R. (2006). Temporal and spatial variation of forest VOC emissions in Germany in the
484 decade 1994–2003. *Atmospheric Environment*, 40, 166-177.

485 Velikova V., Várkonyi Z., Szabó M., Maslenkova L., Nogues I., Kovács L., Peeva V., Busheva M., Garab G. &
486 Sharkey T.D. (2011). Increased thermostability of thylakoid membranes in isoprene-emitting leaves
487 probed with three biophysical techniques. *Plant Physiology*, 157, 905-916.

488 Vlasenko A., Macdonald A., Sjostedt S. & Abbatt J. (2010). Formaldehyde measurements by Proton transfer
489 reaction–Mass Spectrometry (PTR-MS): correction for humidity effects. *Atmospheric Measurement*
490 *Techniques*, 3, 1055-1062.

491 Von Caemmerer S.v. & Farquhar G. (1981). Some relationships between the biochemistry of photosynthesis and
492 the gas exchange of leaves. *Planta*, 153, 376-387.

493 Xie X., Shao M., Liu Y., Lu S., Chang C.-C. & Chen Z.-M. (2008). Estimate of initial isoprene contribution to
494 ozone formation potential in Beijing, China. *Atmospheric Environment*, 42, 6000-6010.

495

496

497

498

499

500

501

502

503

504

505

506

507

508

509

510

511

512

513

514

515

516

517

518 **Table:**

519 **Table 1:** Net photosynthesis (P_n , $\mu\text{molCO}_2 \text{ m}^{-2} \text{ s}^{-1}$), stomatal conductance to water (G_w , $\text{mmolH}_2\text{O m}^{-2} \text{ s}^{-1}$) and emission rates ($\mu\text{gC g}_{\text{DM}}^{-1} \text{ h}^{-1}$) according to treatment and season.
 520 Values represent an average of all data measured between 12h and 15h (local time). Letters denote the difference between drought treatments with a > b and values showed
 521 represent the mean \pm SE, n=5. ND: natural drought and AD: amplified drought with ns = non-significant, (*) = $0.05 < P < 0.1$, * = $0.01 < P < 0.05$, ** = $0.001 < P < 0.01$,

Season	Spring			Summer			Autumn			
	Treatments	ND	AD	P	ND	AD	P	ND	AD	P
Pn		11 \pm 1 a	9 \pm 2 a	ns	14 \pm 2 a	9 \pm 1.2 b	(*)	7 \pm 1 a	9 \pm 1 a	ns
Gw		110 \pm 19 a	57 \pm 13 b	(*)	285 \pm 38 a	126 \pm 17 b	**	122 \pm 23 a	74 \pm 21 a	ns
Isoprene		20 \pm 4 a	10 \pm 2 b	*	124 \pm 10 a	81 \pm 11 b	*	3 \pm 1 a	5 \pm 2 a	ns
MACR+MVK+ISOPOOH		0.1 \pm 0.03a	0.1 \pm 0.01 a	ns	0.4 \pm 0.1 a	0.2 \pm 0.02 b	*	0.04 \pm 0.01 a	0.1 \pm 0.01 a	ns
Methanol		1 \pm 0.1 a	0.5 \pm 0.04 b	*	1 \pm 0.2 a	0.6 \pm 0.03 b	*	0.2 \pm 0.03 a	0.2 \pm 0.1 a	ns
Acetaldehyde		1 \pm 0.4 a	1 \pm 0.3 a	ns	2 \pm 0.5 a	1 \pm 0.1 a	ns	1 \pm 0.3 a	1 \pm 0.3 a	ns
Acetone		0.5 \pm 0.1 a	0.2 \pm 0.02 a	ns	1 \pm 0.2 a	0.5 \pm 0.04 b	**	0.4 \pm 0.1 a	0.4 \pm 0.1 a	ns
Formaldehyde		0.2 \pm 0.05 a	0.1 \pm 0.01 a	ns	0.4 \pm 0.1 a	0.1 \pm 0.02 b	**	0.2 \pm 0.1 a	0.3 \pm 0.1 a	ns

522

523 **Figure legends**

524 **Figure 1:** Ombrothermic diagram for natural and amplified drought in 2012, 2013 and 2014. Bars represent mean
525 monthly precipitation (mm) and curves represent mean monthly temperature (°C). On each amplified drought
526 graph, the percentage represents the proportion of excluded rain compared to the natural drought plot.

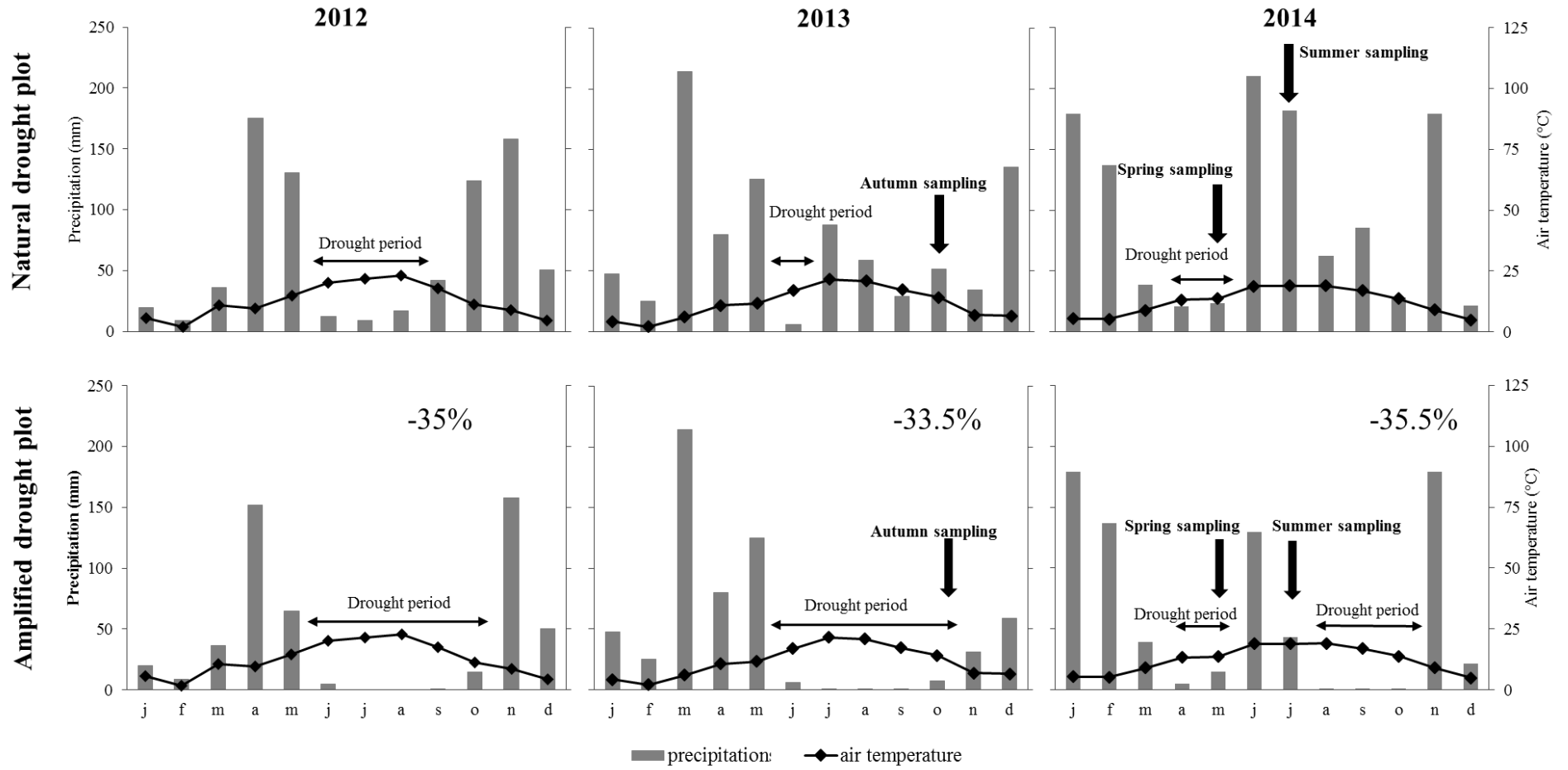
527
528 **Figure 2:** Diurnal pattern of stomatal conductance (G_w) and net photosynthesis (P_n) according to drought
529 treatment and season. Values showed represent means \pm SE, n=5.

530
531 **Figure 3:** Diurnal pattern of isoprene emissions rates, where points represent measured emission and the yellow
532 line corresponds to modelled emissions rates according to the $L+T$ algorithm (ER_{L+T}). R^2 and slope (sl) of
533 correlations between measured (x axis) and modelled (y axis) emissions are presented in the yellow frame.
534 Correlations were obtained without forcing data to pass through the origin. Values are mean \pm SE, n=5.

535
536 **Figure 4:** Diurnal pattern of acetaldehyde emissions rates, where points represent measured emission, the yellow
537 line corresponds to modelled emissions rates according to the $L+T$ algorithm (ER_{L+T}) and the dotted line
538 corresponds to modelled emissions rates according to the T algorithm (ER_T). R^2 and slope (sl) of correlations
539 between measured (x axis) and modelled (y axis) emissions are presented in the yellow frame for $L+T$ and in the
540 white frame for T . Correlations were obtained without forcing data to pass through the origin. Values are mean \pm
541 SE, n=5.

542
543 **Figure 5:** Diurnal pattern of measured methanol emissions rates. Points represent measured emission, the yellow
544 line corresponds to modelled emissions rates according to the $L+T$ algorithm (ER_{L+T}) and the dotted line
545 corresponds to modelled emissions rates according to the T algorithm (ER_T). R^2 and slope (sl) of correlations
546 between measured (x axis) and modelled (y axis) emissions are presented in the yellow frame for $L+T$ and in the
547 white frame for T . Correlations were obtained without forcing data to pass through the origin. Values are mean \pm
548 SE, n=5.

549
550
551
552
553
554
555

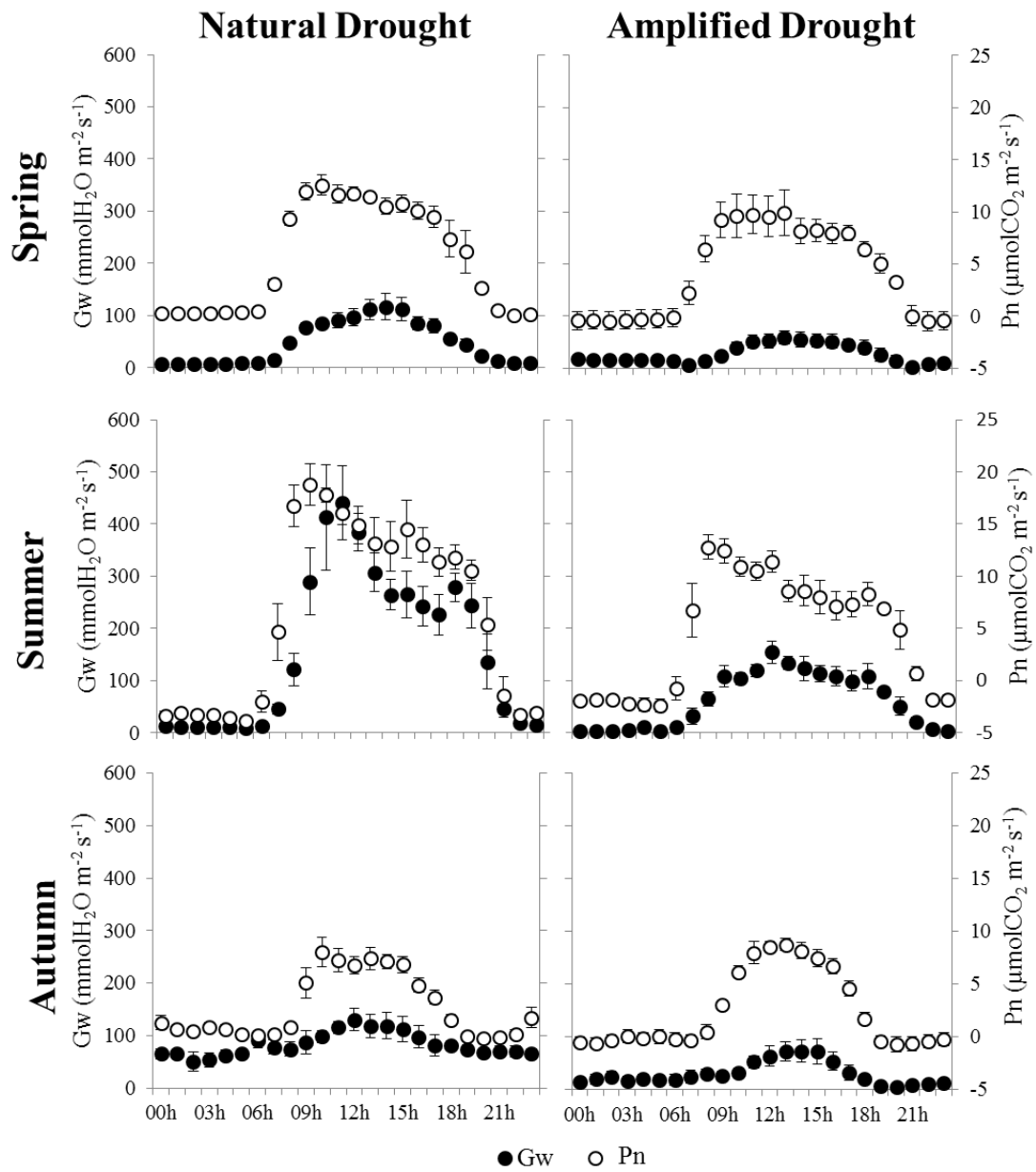


556

557 **Figure 1:**

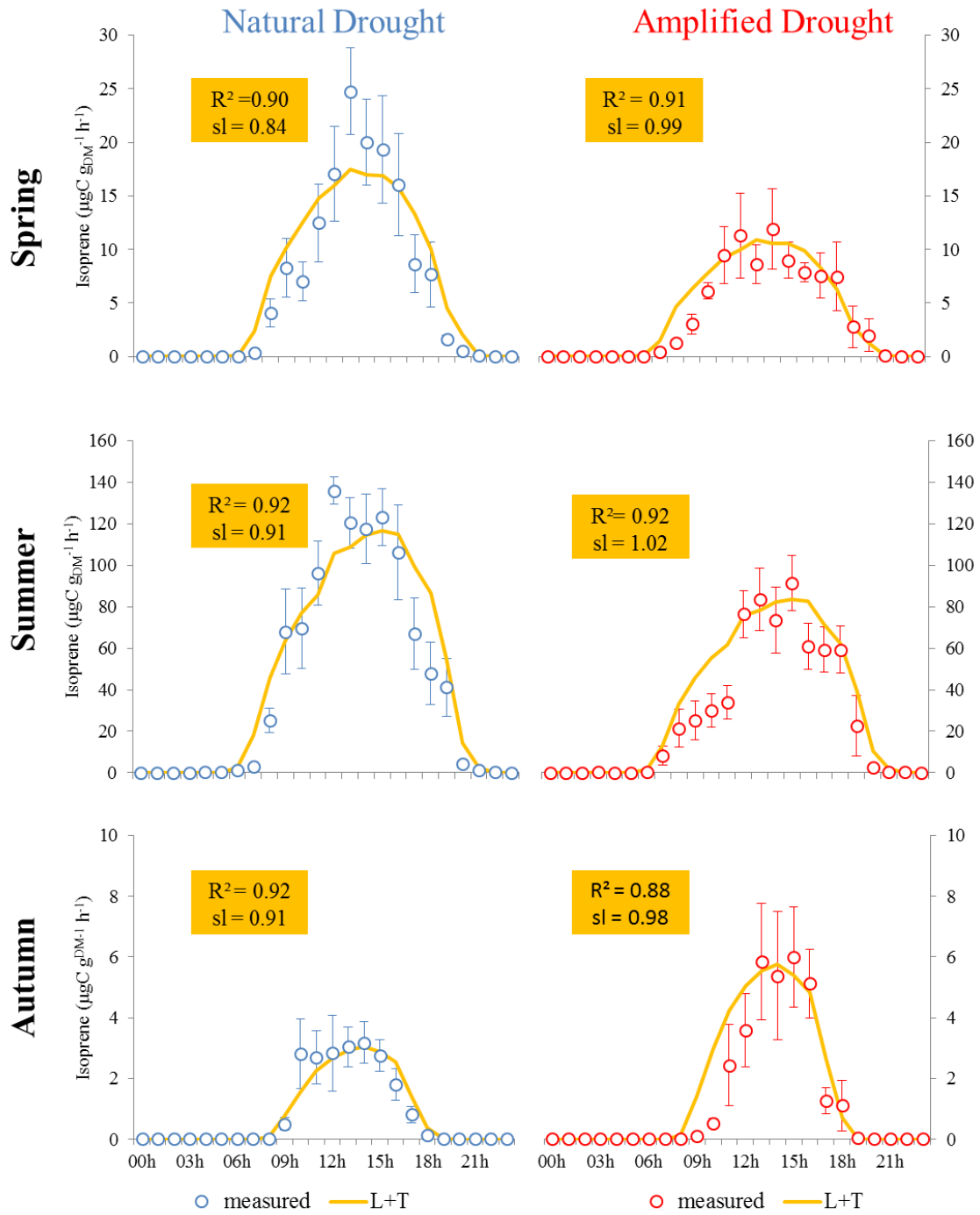
558

559



561

562 **Figure 2:**

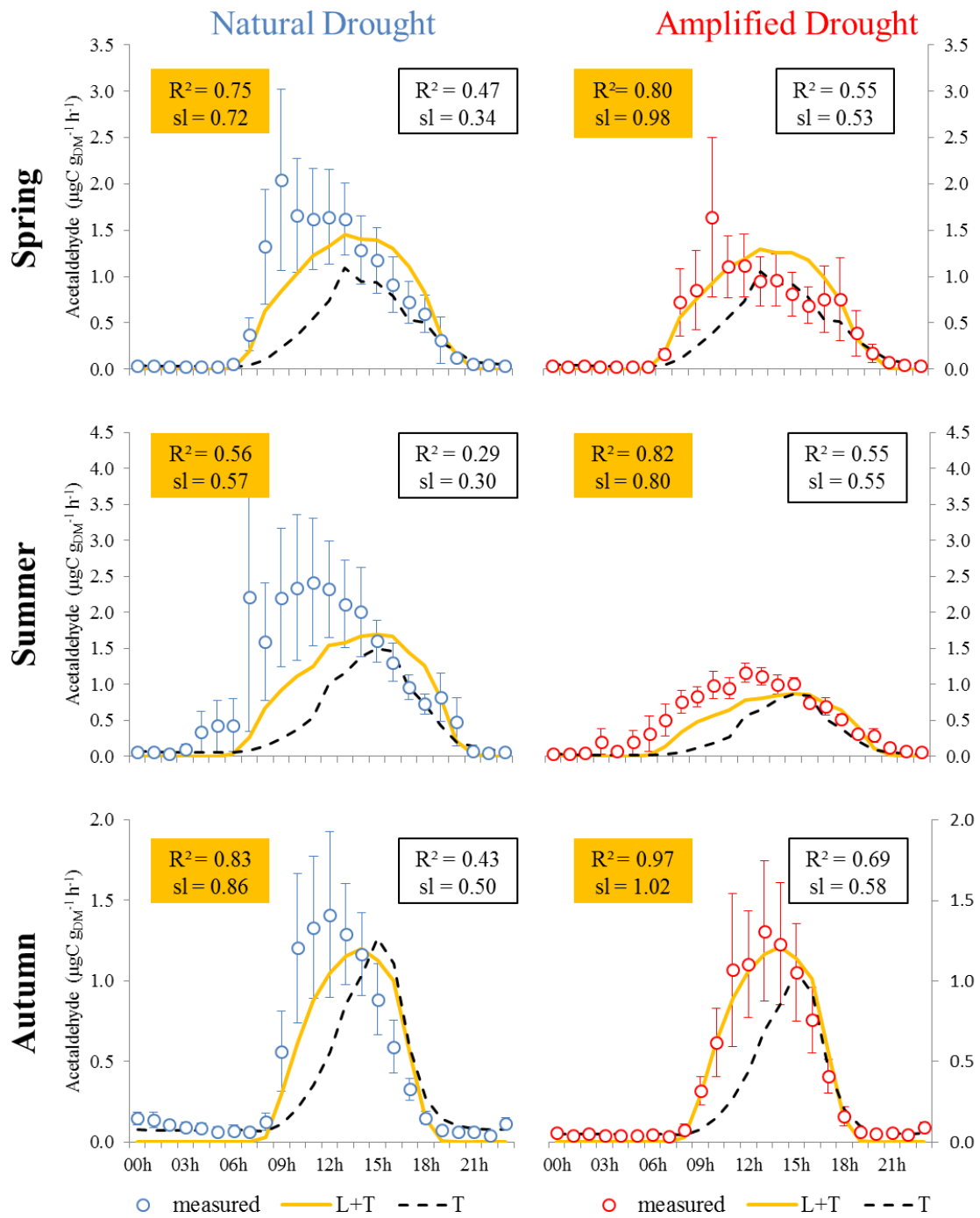


563

564 **Figure 3:**

565

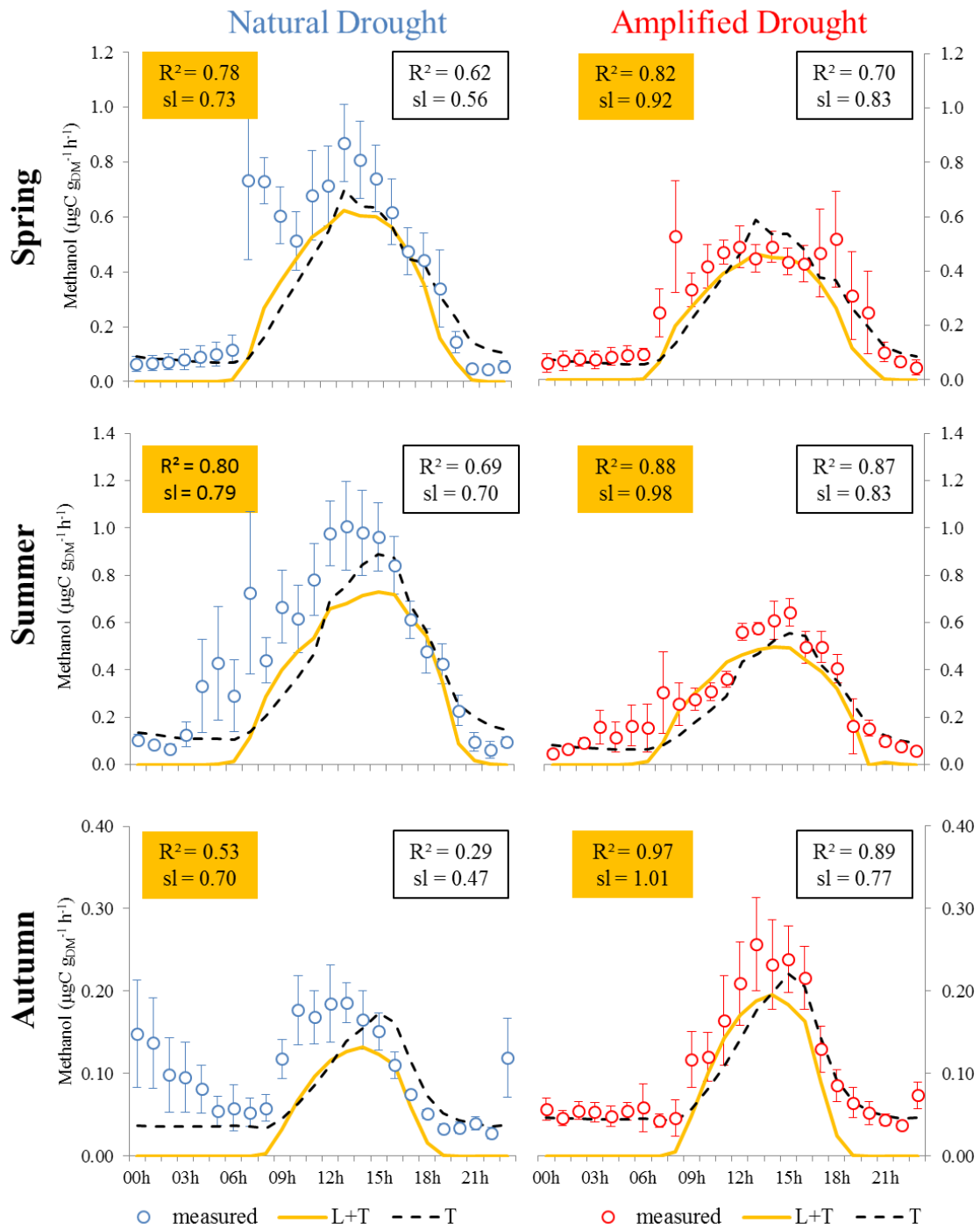
566



567

568 **Figure 4:**

569



570

571 **Figure 5:**

572

573

574

575

576